

The stress–strain rate behaviour of superplastic Zn–Al eutectoid alloy

R. S. MISHRA*, G. S. MURTY

Department of Metallurgical Engineering, Indian Institute of Technology, Kanpur, India

The stress–strain rate behaviour of a superplastic Zn–22% Al alloys was investigated by the differential strain rate and constant load cycling tests on an Instron machine. A region with a rate sensitivity approaching unity was observed at low strain rates. On increasing the strain rate, a transition to the superplastic region occurred through an intermediate region of lower m (~ 0.35). These observations are interpreted in terms of a transition from diffusional creep to superplastic flow with a threshold stress for superplastic deformation.

1. Introduction

In general, it has been established that the logarithmic plots of stress (σ) against strain rate ($\dot{\epsilon}$) for superplastic materials are sigmoidal in nature. Despite this observation in most of the materials, the nature of the curve for the Zn–Al eutectoid at low strain rates is still not clear. Varying trends of both an increase and a decrease in rate sensitivity index (m) were observed by different investigators. The increase in m at low strain rates (region 1) observed first by Vaidya *et al.* [1] was subsequently confirmed by Mukherjee and co-workers [2–4]. This observation was attributed to diffusional creep. Contrary to this observation, other workers observed a decrease in the m value in region 1 [5–14]. This was interpreted as an unidentified separate mechanism [5]. Vale *et al.* [11] observed an increase in m at very low stresses (region 0) below those of the normal region 1. These differences in observations were treated by many reviewers [15–18]. Different explanations were put forward to suggest that each of these observations is a spurious one. Grivas *et al.* [16] suggested that the observed increase in m at low strain rates could be a consequence of primary creep. It was argued that the measured creep rate in the experiments where a high m value was observed, was overestimated because steady state was not attained in their creep tests. On the other hand, it was suggested by Arieli and Mukherjee [15, 17] that the decrease in m value at low strain rates could be the result of concurrent grain growth. They showed that at constant strain rate concurrent grain growth could lead to a higher flow stress at low strain rates. Arieli and Mukherjee [17] have suggested that region 1 controversy might be due to different thermomechanical history of the alloy. However, Logan and Mukherjee [13] did not observe any effect of prior thermomechanical treatment in region 1 and confirmed that the low m value region exists even after grain-growth correction. Furthermore, the effect of concurrent grain growth on the stress–strain rate data depends on the test procedure and it does not always lead to a decrease in m .

The observations of various investigators on the Zn–Al eutectoid alloy are summarized in Table I. The present study was aimed at re-evaluating the shape of the true stress–true strain rate curve for steady state deformation in the absence of any grain growth during the tests.

2. Experimental procedure

The Zn–22 wt % Al alloy was prepared from 99.99% pure zinc and 99.9% pure aluminium. An ingot, 14 mm thick, was cast, homogenized and hot rolled at 300°C to 1.8 mm thickness. Tensile specimens of 20 mm gauge length and 5 mm width were machined out of the hot-rolled material. The specimens were annealed at 350°C for 20 h, quenched in water and then annealed at 250°C for varying times to obtain different grain sizes. Finally the specimens were subjected to a standard prestrain of $\sim 30\%$ at 230°C at a

TABLE I Summary of the reported parameters of the constitutive equation for the Zn–Al eutectoid alloy

Region	Activation energy Q (kJ mol ⁻¹)	Grain size exponent, p	Stress exponent, $n = 1/m$	Reference	
1	74.4	2.5 \pm 0.32	0.87 \pm 0.12	[1]	
	64.4 \pm 6.0	3.0	1.0	[2]	
	95.9 \pm 2.1	2.0 \pm 0.1	1.0	[3]	
	42.7	2.5	1.25 (Finer d)	[4]	
	118.3	1.6	1.0 (Coarser d)	[4]	
	119.0	2.4	3.8	[5, 7]	
	83.7	–	3.0	[6]	
	89.0	2.8	3.1	[11]	
	123 \pm 10	2.4	3.1	[13]	
	159.0	–	4.0–5.0	[14]	
	2	79.0	1.69 \pm 0.29	1.99 \pm 0.15	[1]
		64.6 \pm 6.0	2.0	2.0	[2]
		69.9	2.0	2.2	[3]
		54.8	2.2	2.0	[4]
78.8		2.4	2.2	[5, 7]	
54.4		–	2.0	[6]	
74.0		–	2.4	[11]	
73.0–94.0		2.3–2.6	1.8–2.3	[13]	
80.0		–	2.4	[14]	

* Present address: Department of Metallurgy, University of Sheffield, UK.

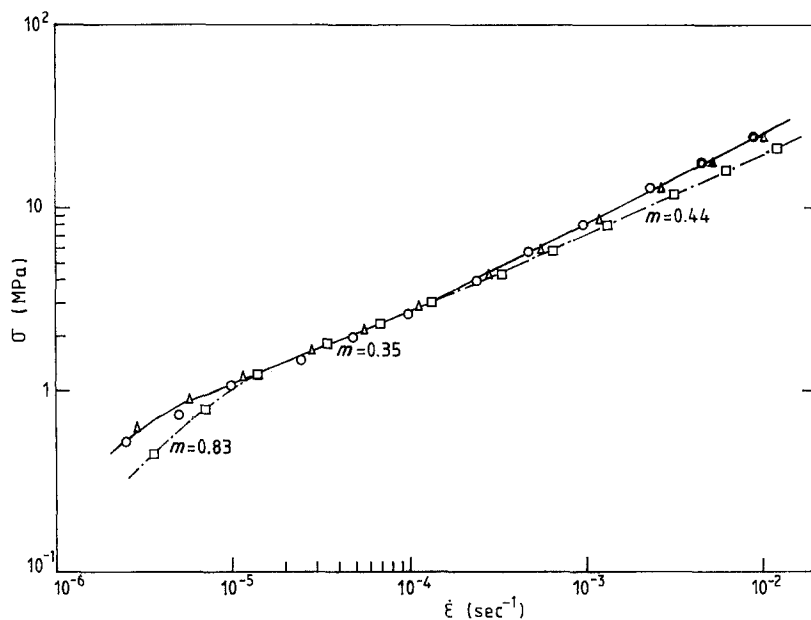


Figure 1 Effect of repeated strain rate cycling on the stress-strain rate behaviour (m values refer to the first cycle data). (\square) Cycle I, (Δ) cycle II, (\circ) cycle III; $d = 1.9 \mu\text{m}$, $T = 230^\circ\text{C}$.

cross-head speed of 1.0 mm min^{-1} using an Instron machine. The stress-strain rate data were obtained by the differential strain rate and constant load cycling tests on an Instron machine. An oil bath with a temperature control of $\pm 1^\circ\text{C}$ was employed for the test temperature range of 140 to 230°C . Differential strain rate tests were carried out mostly in the increasing order of cross-head speeds starting from the lowest cross-head speed of $0.005 \text{ mm min}^{-1}$. Constant load tests were performed on the same specimen following the differential strain rate test. The straining in each case was continued to ensure steady state flow.

Optical metallography was carried out to evaluate the grain size before and after each test. Both gauge and shoulder sections were examined to determine the effect of deformation on grain growth. The grain size (d) reported here is $1.78\bar{l}$, where \bar{l} is the mean linear intercept length.

3. Results

The σ - $\dot{\epsilon}$ plots of Fig. 1 were obtained by performing three cycles of differential strain rate test at 230°C on

a single specimen without any prestrain. Comparison of the first and second cycle data indicates that the stress in the second cycle data is slightly higher both in the lower and higher strain rate range. However, the second and third cycle data are nearly identical, despite the fact that the third cycle data were obtained following the decremental sequence of cross-head speeds. Thus the stress-strain rate data are unique (independent of path of loading) after some initial prestrain. In order to avoid this initial strain effect on flow stress, all specimens were subjected to a standard prestrain. Another feature of the data shown in Fig. 1 concerns the shape of the stress-strain rate plot. Starting from the highest strain rate range, it can be seen that the strain rate sensitivity index decreases to a minimum of ~ 0.35 before it increases again at the lower end of the strain rate range. Hereafter, the lower strain rate region of this study, where m is high, will be referred to as region 1.

Fig. 2 shows the stress-strain rate plots for the $2.1 \mu\text{m}$ grain size. The variation in the rate sensitivity with strain rate of these data is illustrated in Fig. 3.

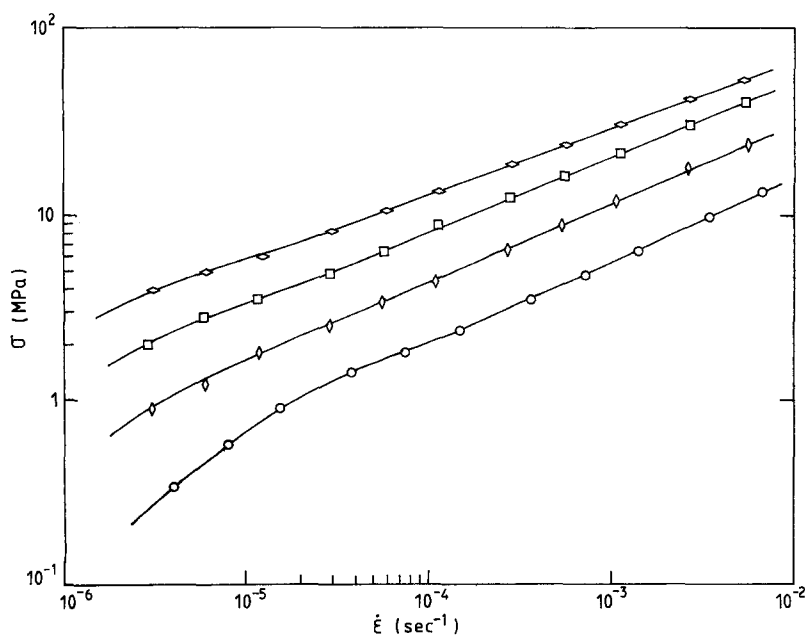


Figure 2 Stress-strain rate plots for a grain size of $2.1 \mu\text{m}$. $T = (\odot)$ 140°C , (\square) 170°C , (Δ) 200°C , (\circ) 230°C .

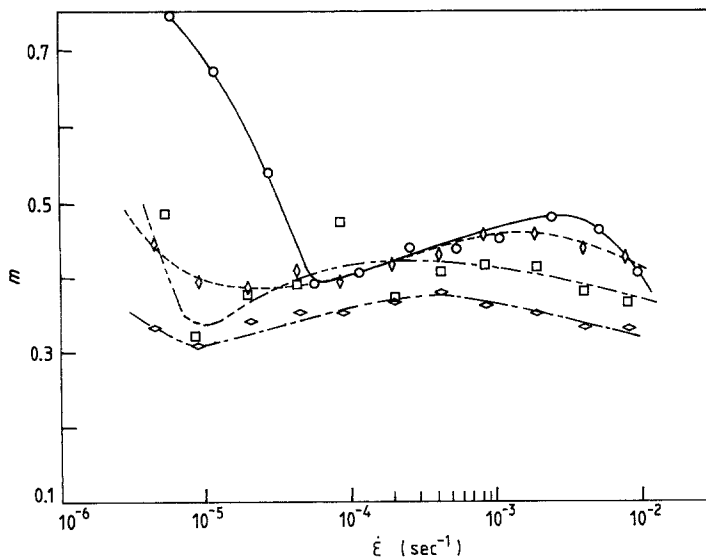


Figure 3 Variation of strain rate sensitivity index with strain rate ($d = 2.1 \mu\text{m}$). $T = (\diamond) 140^\circ\text{C}$, $(\square) 170^\circ\text{C}$, $(\triangle) 200^\circ\text{C}$, $(\circ) 230^\circ\text{C}$.

Additional stress–strain rate plots for two other grain sizes are given in Figs 4 and 5. It may be noted that region 1 of high m is less conspicuous within the investigated strain rate range as the grain size increases or the test temperature decreases. The grain-size data obtained from the microstructural observations before and after the differential strain rate test at 230°C are presented in Table II. The deformation-induced grain coarsening can be noted to be negligibly small.

The grain size (d) dependence of strain rate and the activation energy (Q) for flow were determined making use of the following constitutive equation:

$$\dot{\epsilon} = (AD_0Eb/kT)(b/d)^p(\sigma/E)^n \exp(-Q/RT) \quad (1)$$

where A is a dimensionless constant, D_0 is the pre-exponential factor in diffusivity, E is the modulus of elasticity, b is the Burger's vector, k is the Boltzmann constant, R is the gas constant, T is the temperature and $n (= 1/m)$ is the stress exponent. From plots of $\log(\dot{\epsilon}/\sigma^n)$ against $\log d$ at different temperatures shown in Fig. 6, a representative value of p in region 2 is 3.8 ± 0.53 . In region 1, the value of p could only be estimated at 230°C and it is 3.93 ± 0.47 . The Arrhenius plots for region 2 are shown in Fig. 7 and the mean value of activation energy is 94.1 kJ mol^{-1} . The activation energy for region 1 estimated from the data of one grain size is $85.9 \pm 11.7 \text{ kJ mol}^{-1}$.

4. Discussion

The σ – $\dot{\epsilon}$ data of this study indicates a transition from a region of high m (approaching unity) to a superplastic region with $m = 0.5$. This transition is accompanied by a low m (~ 0.35) region at an intermediate strain

rate range. The observation of high m region at low strain rates is in agreement with the data of one group of workers [1–4]. The intermediate region of low m can be noted to be similar to the region 1 of low m reported by the other group of workers [5–14]. A similar trend of both an increase and a decrease in m with increasing strain rate at the lower end of the strain rate range was also observed in two other studies [11, 14].

Rai and Grant [19] considered the effect of concurrent grain growth and showed that it can lead to a false low m value region. However, this is valid only when different test specimens are used for each datum point. The concurrent grain-growth effect in the Zn–22% Al alloy was discussed in detail [15–18], but no distinction was made between the data obtained by stress or strain rate cycling technique on a single specimen with different specimens. Mishra and Murty [20] examined the effect of concurrent grain growth on data obtained by strain rate or stress cycling technique. They showed that concurrent grain growth during incremental strain rate or stress cycling leads to an apparent increase in m , contrary to the argument used earlier [15–18]. On the other hand, during decremental strain rate cycling, concurrent grain growth lowers the m value. Moreover, a unique σ – $\dot{\epsilon}$ behaviour that is independent of the path of loading implies negligible grain growth during the test cycles. In the present study, both incremental and decremental step sequence of strain rates in a differential strain rate test resulted in an identical σ – $\dot{\epsilon}$ relation, as shown in Fig. 1. The grain-size measurements before and after testing also indicate negligible grain growth. Thus the observed variations of m cannot be a consequence of deformation-induced coarsening. The same argument would be applicable to the data of Mohamed *et al.* [5, 7].

Grivas *et al.* [16] have examined the role of primary creep and showed that a high m value region can arise if the data do not correspond to a steady state. They also pointed out the conflicting reports by Vaidya *et al.* [1] and Arieli *et al.* [3], who observed transient creep, whereas Misro and Mukherjee [2] did not observe any transient creep. In the present study, an increase in m value was observed at low strain rates in

TABLE II Grain-size data resulting from deformation at 230°C

Initial grain size (μm)	Elongation (%)	Grain size after deformation (μm)	Grain size in shoulder region (μm)
2.1 ± 0.5	89	2.2 ± 0.5	—
3.1 ± 1.1	45	3.4 ± 0.6	3.0 ± 0.6
3.6 ± 0.7	48	3.7 ± 0.9	3.6 ± 0.7
4.4 ± 1.4	61	5.0 ± 1.3	4.4 ± 0.9

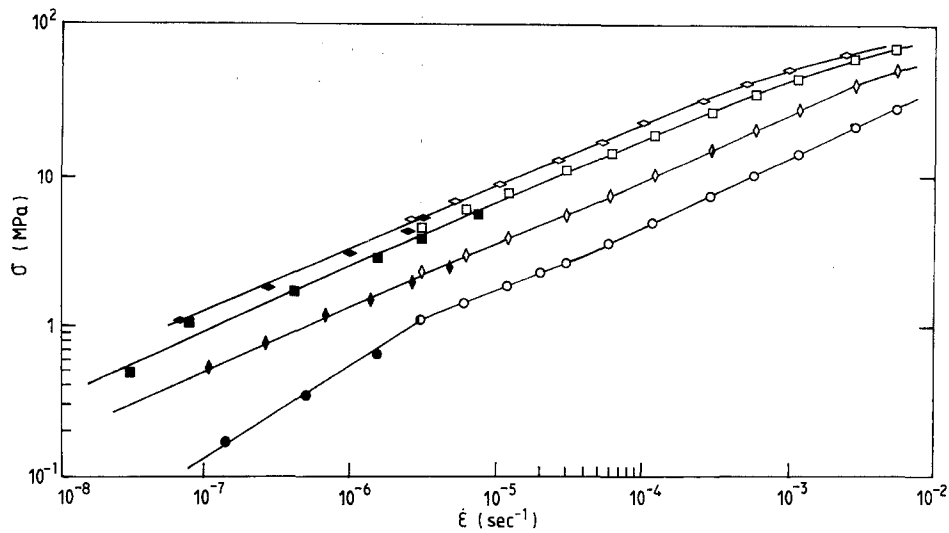


Figure 4 Stress-strain rate plots for a grain size of $3.1 \mu\text{m}$. Open symbols, $\dot{\epsilon}$ change; solid symbols, creep. $T = (\diamond, \blacklozenge)$ 140°C , (\square, \blacksquare) 170°C , $(\triangle, \blacktriangle)$ 200°C , (\circ, \bullet) 230°C .

specimens tested by constant cross-head speed tests and constant load tests, where the strain increments corresponding to each datum point were sufficiently large to ensure steady state deformation. Thus the primary creep effect cannot be the reason for the observed trends of this study.

While the observed regions of low and high m values in various studies on the Al-22% Zn alloy at strain rates below those of region 2 are not spurious effects of grain growth or primary creep, their prominence varies in different investigations. The reason for the variations in the observations under apparently similar experimental conditions needs to be considered. At low strain rates, the m value tending towards unity and an activation energy close to that of lattice diffusion in zinc suggest that diffusional creep (Nabarro-Herring) becomes dominant as an independent mechanism. As the strain rate is increased, transition to the superplastic region with an m value of 0.5 occurs. If a threshold stress exists for superplastic flow, this transition is accompanied by a decrease in the rate sensitivity of flow stress. Mohamed [21] analysed some of the pre-

vious data in terms of a threshold stress, which may result from impurity atom segregation at boundaries and their interaction with boundary dislocations. According to this suggestion, the magnitude of the threshold stress would depend on the impurity content of the alloy. If the Zn-Al eutectoid alloy is prepared starting from high-purity metals, the threshold stress arising from impurity segregation at boundaries will be minimal. On the other hand, the threshold stress will be significantly higher if commercial alloys are investigated. Accordingly, depending on the impurity content and thus the threshold stress, the transition from diffusional flow to superplastic flow on increasing the strain rate will be accompanied by a region of varying m . In the absence of a threshold stress, the transition from an m value of unity to 0.5 will be without any intermediate region. When the threshold stress is significant, the intermediate region of low m value will be prominent. The variations of observations among different investigators can thus be linked to the purity of the starting materials.

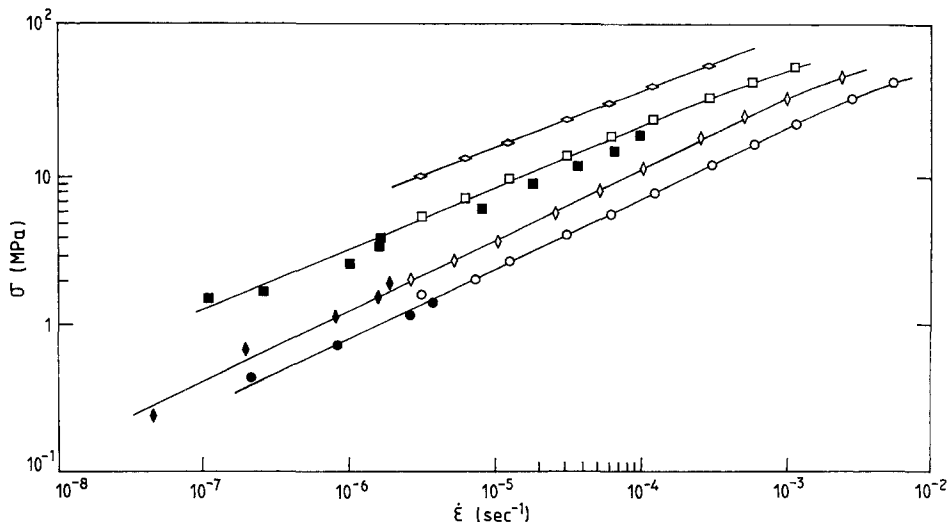


Figure 5 Stress-strain rate plots for a grain size of $4.4 \mu\text{m}$. Open symbols, $\dot{\epsilon}$ change; solid symbols, creep. $T = (\diamond, \blacklozenge)$ 140°C , (\square, \blacksquare) 170°C , $(\triangle, \blacktriangle)$ 200°C , (\circ, \bullet) 230°C .

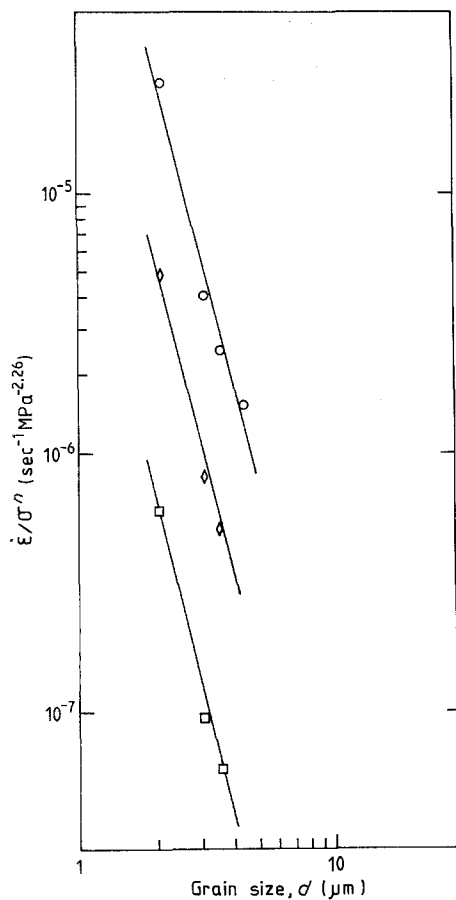


Figure 6 Cross-plot for the determination of the grain size exponent in region 2. $\sigma = 10$ MPa. (\square) 170°C , $p = 3.41 \pm 0.48$; (\diamond) 200°C , $p = 4.20 \pm 0.50$; (\circ) 230°C , $p = 3.86 \pm 0.53$.

5. Conclusions

A region of high strain rate sensitivity approaching unity is observed at low strain rates. As the strain rate increases, m decreases to ~ 0.35 before it attains a value of 0.5, which is characteristic of the superplastic region. Neither concurrent grain growth nor transient creep phenomena can account for these observations. An impurity-dependent threshold stress for superplastic flow appears to be responsible for the variations in observations among various investigators.

References

1. M. L. VAIDYA, K. L. MURTY and J. E. DORN, *Acta Metall.* **21** (1973) 1615.
2. S. C. MISRO and A. K. MUKHERJEE, in "Rate Processes in Plastic Deformation of Materials", edited by J. C. M. Li and A. K. Mukherjee (ASM, Cleveland, Ohio, 1975) p. 434.
3. A. ARIELI, A. K. S. YU and A. K. MUKHERJEE, *Met. Trans.* **11A** (1980) 181.
4. A. ARIELI and A. K. MUKHERJEE, *Acta Metall.* **28** (1980) 1571.

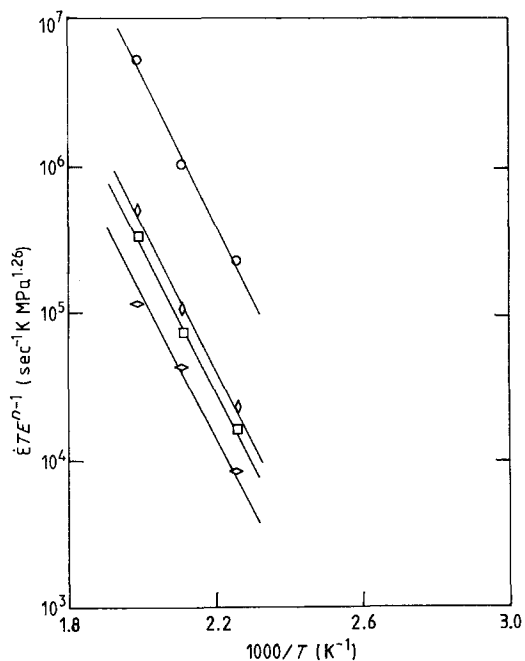


Figure 7 Arrhenius plot for the determination of the activation energy for flow in region 2. $\sigma = 10$ MPa. (\circ) $d = 2.1 \mu\text{m}$, $Q = 98.7 \pm 13.4 \text{ kJ mol}^{-1}$; (\diamond) $d = 3.1 \mu\text{m}$, $Q = 97.5 \pm 13.2 \text{ kJ mol}^{-1}$; (\square) $d = 3.6 \mu\text{m}$, $Q = 98.4 \pm 13.3 \text{ kJ mol}^{-1}$; (\diamond) $d = 4.4 \mu\text{m}$, $Q = 81.9 \pm 11.1 \text{ kJ mol}^{-1}$.

5. F. A. MOHAMED and T. G. LANGDON, *ibid.* **23** (1975) 117.
6. H. NAZIRI, R. PEARCE, M. H. BROWN and K. F. HALE, *ibid.* **23** (1975) 489.
7. F. A. MOHAMED, S. A. SHEI and T. G. LANGDON, *ibid.* **23** (1975) 1443.
8. F. A. MOHAMED, M. M. I. AHMED and T. G. LANGDON, *Met. Trans.* **8A** (1977) 933.
9. D. GRIVAS, Rep. LBL-7375, 1978 (Lawrence Berkeley Laboratory, University of California, Berkeley).
10. P. SHRIAT, R. B. VASTAVA and T. G. LANGDON, *Acta Metall.* **30** (1982) 285.
11. S. H. VALE, D. J. EASTGATE and P. M. HAZZLEDINE, *Scripta Metall.* **13** (1979) 1157.
12. D. W. LIVESEY and N. RIDLEY, *ibid.* **16** (1982) 165.
13. R. W. LOGAN and A. K. MUKHERJEE, *Mater. Sci. Engng* **54** (1982) 237.
14. G. S. MURTY, *Scripta Metall.* **20** (1986) 533.
15. A. ARIELI and A. K. MUKHERJEE, *ibid.* **13** (1979) 331.
16. D. GRIVAS, J. W. MORRIS Jr and T. G. LANGDON, *ibid.* **15** (1981) 229.
17. A. ARIELI and A. K. MUKHERJEE, *ibid.* **15** (1981) 237.
18. R. W. LOGAN, *ibid.* **16** (1982) 845.
19. G. RAI and N. J. GRANT, *Met. Trans.* **6A** (1975) 385.
20. R. S. MISHRA and G. S. MURTY, *J. Mater. Sci. Lett.* (1988) in press.
21. F. A. MOHAMED, *J. Mater. Sci.* **18** (1983) 582.

Received 1 April
and accepted 16 June 1987